

Putative quantum critical point in the itinerant magnet ZrFe_4Si_2 with a frustrated quasi-one-dimensional structure

M. O. Ajeesh,* K. Weber, C. Geibel, and M. Nicklas

Max Planck Institute for Chemical Physics of Solids, Nöthnitzer Str. 40, 01187 Dresden, Germany

(Dated: November 19, 2020)

The Fe sublattice in the compound ZrFe_4Si_2 features geometrical frustration and quasi-one-dimensionality. We therefore investigated the magnetic behavior in ZrFe_4Si_2 and its evolution upon substituting Ge for Si and under the application of hydrostatic pressure using structural, magnetic, thermodynamic, and electrical-transport probes. Magnetic measurements reveal that ZrFe_4Si_2 holds paramagnetic Fe moments with an effective moment $\mu_{\text{eff}} = 2.18 \mu_B$. At low temperatures the compound shows a weak short-range magnetic order below 6 K. Our studies demonstrate that substituting Ge for Si increases the unit-cell volume and stabilizes the short-range order into a long-range spin-density wave type magnetic order. On the other hand, hydrostatic pressure studies using electrical-resistivity measurements on $\text{ZrFe}_4(\text{Si}_{0.88}\text{Ge}_{0.12})_2$ indicate a continuous suppression of the magnetic ordering upon increasing pressure. Therefore, our combined chemical substitution and hydrostatic pressure studies suggest the existence of a lattice-volume-controlled quantum critical point in ZrFe_4Si_2 .

I. INTRODUCTION

Itinerant magnetic systems with low dimensionality and magnetic frustration exhibit enhanced quantum fluctuations leading to the emergence of novel and exotic phases displaying unconventional behaviors. Studying such systems is of great importance as it is becoming increasingly evident that quantum fluctuations play a crucial role in emergent phenomena, including unconventional superconductivity and unconventional metallic phases¹⁻⁹. In order to improve our understanding of these phenomena and the importance of dimensionality and frustration on the ground-state properties investigations of new candidate materials are highly desired.

In this regard, ternary intermetallic AFe_4X_2 (A = rare earth, X = Si, Ge) compounds are interesting candidates due to their peculiar crystal structure. These compounds crystallize in the ZrFe_4Si_2 -type structure with the $P4_2/mnm$ space group at room temperature¹⁰. The crystal structure consists of slightly distorted Fe tetrahedra, which are edge shared to form chains along the crystallographic c axis, as illustrated in Fig. 1. The Fe tetrahedra are prone to magnetic frustration, and the chainlike arrangement provides the quasi-one-dimensional character of the magnetic system, rendering the AFe_4X_2 compounds excellent candidate materials to study quantum fluctuations and their effect on the physical properties in low-dimensional frustrated systems.

Previous studies on the AFe_4X_2 family mostly focused on compounds with magnetic rare-earth ions A . Low-temperature neutron and x-ray diffraction studies on $(\text{Er}, \text{Dy}, \text{Ho}, \text{Tm})\text{Fe}_4\text{Ge}_2$ revealed that the compounds undergo antiferromagnetic ordering at low temperatures resulting in complex spin arrangements due to competing interactions between the magnetic rare-earth and Fe sublattices¹¹⁻²¹. In all of the compounds, the magnetic ordering is accompanied by a structural transition from tetragonal to orthorhombic symmetry. AFe_4X_2 compounds with nonmagnetic rare-earth elements are even

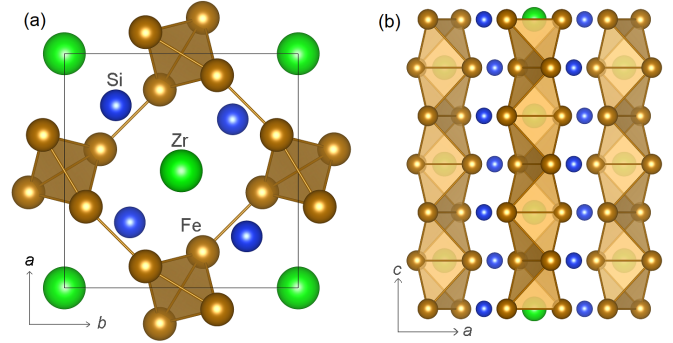


FIG. 1: (a) Crystal structure of ZrFe_4Si_2 viewed along the crystallographic c axis. (b) The chainlike arrangement of edge-shared Fe tetrahedra viewed along the b axis.

less investigated as only powder neutron diffraction studies on YFe_4Ge_2 , LuFe_4Ge_2 , and YFe_4Si_2 have been reported^{22,23}. These compounds also order antiferromagnetically at low temperatures with a simultaneous structural transition from tetragonal $P4_2/mnm$ to orthorhombic $Pnmm$ symmetry. While the existing studies address the magnetic structure and the magneto-elastic transitions in these compounds, there are no reports on tuning the magnetic to a non-magnetic ground state by an external control parameter.

In this paper, we present an investigation on a member of the 142 family: ZrFe_4Si_2 . Replacing the rare-earth ions with Zr not only reduces the lattice volume but also changes the valency of the A ion from 3+ to 4+. This may lead to a significant change in the electronic structure and, therefore, of the ground state compared to rare-earth-containing 142 compounds. Here, we studied the ground-state properties of ZrFe_4Si_2 using magnetic, thermodynamic, and electrical-transport measurements on polycrystalline samples. Our results reveal short-range magnetic ordering below 6 K which is stabilized into a spin-density wave (SDW) long-range order by

substituting Ge on Si sites. In addition, we applied external hydrostatic pressure on $\text{ZrFe}_4(\text{Si}_{0.88}\text{Ge}_{0.12})_2$ to tune the antiferromagnetically ordered ground state toward a nonmagnetic state. Finally, we discuss the temperature–lattice-volume phase diagram in which the magnetic ordering is suppressed by decreasing lattice volume toward a putative quantum critical point (QCP).

II. METHODS

Polycrystalline samples of ZrFe_4Si_2 were synthesized by a standard arc-melting technique on a copper hearth. At first stoichiometric amounts of the constituent elements (at least 99.9% purity) were melted in an arc furnace under argon atmosphere, followed by several flipping and remelting of the resulting ingot to ensure homogeneity. Then the as-cast samples were annealed at 1150°C under a static argon atmosphere for a week. The phase purity of the annealed samples was checked by powder x-ray diffraction (PXRD) using Cu K_α radiation and a scanning electron micrograph (SEM). Energy dispersive x-ray (EDX) analysis was used to check the stoichiometry of the samples. SEM studies reveal only a small amount (up to 2%) of eutectic phase Fe_3Si in our samples, enabling us to study the intrinsic properties of ZrFe_4Si_2 . PXRD patterns confirm the tetragonal $P4_2/mnm$ structure type with lattice parameters $a = 6.9916(5) \text{ \AA}$ and $c = 3.7551(5) \text{ \AA}$, in good agreement with those reported in the literature¹⁰. Polycrystalline samples of the substitution series $\text{ZrFe}_4(\text{Si}_{1-x}\text{Ge}_x)_2$ were also synthesized following the same procedure. EDX analysis provides the Ge concentrations in the obtained samples as $x = 0.12$ (0.1), 0.23 (0.2), 0.34 (0.3), and 0.46 (0.4), where the corresponding nominal Ge concentrations used in the synthesis are given in the parantheses. SEM studies revealed that these samples contain up to 5% of impurity phases mainly consisting of $\text{Fe}_3(\text{Si}_{1-x}\text{Ge}_x)$.

DC magnetization measurements were carried out in the temperature range between 1.8 and 300 K and in magnetic fields up to 7 T using a superconducting quantum interference device magnetometer (magnetic property measurement system, Quantum Design). The specific heat was recorded by a thermal-relaxation method using a physical property measurement system (PPMS; Quantum Design). The electrical transport experiments were carried out in the temperature range between 2 and 300 K and magnetic field up to 7 T also using a PPMS. The electrical resistivity was measured using a standard four-terminal method, where electrical contacts to the sample were made using $25 - \mu\text{m}$ gold wires and silver paint.

Electrical-resistivity measurements on $\text{ZrFe}_4(\text{Si}_{0.88}\text{Ge}_{0.12})_2$ under hydrostatic pressure were performed using a double-layered piston-cylinder-type pressure cell with silicon oil as the pressure transmitting medium. The pressure inside the sample space was determined at low temperatures by the shift of the

superconducting transition temperature of a piece of Pb. Electrical resistivity was measured using an LR700 resistance bridge (Linear Research) working at a measuring frequency of 16 Hz.

III. EXPERIMENTAL RESULTS

A. Physical properties of ZrFe_4Si_2

In order to understand the ground-state properties of ZrFe_4Si_2 , we have carried out magnetic, thermodynamic, and electrical-resistivity measurements. The temperature dependence of the DC magnetic susceptibility $\chi(T)$ is shown in Fig. 2a. We note that our ZrFe_4Si_2 samples contain up to 2% eutectic phase Fe_3Si , which orders ferromagnetically above 800 K. Accordingly, this impurity phase induces in the magnetization a ferromagnetic (FM) contribution which, however, saturates at low fields and is therefore field and temperature independent above 1 T and below 300 K, respectively²⁴. Thus, the impurity contribution can easily be separated from the intrinsic contribution of ZrFe_4Si_2 . Using magnetization measurements at different fields, this contribution (M_{FM}) is found to be rather small with a saturation moment of the order of $1 \times 10^{-4} \mu_B/\text{Fe}$. M_{FM} is then subtracted from the measured magnetization to obtain the intrinsic susceptibility as $\chi(T) = [M(T) - M_{\text{FM}}]/H$. At high temperatures, $\chi(T)$ follows a Curie-Weiss behavior $\chi(T) = C/(T - \theta_W)$, where C and θ_W are the Curie constant and the Weiss temperature, respectively. A Curie-Weiss fit to the $\chi^{-1}(T)$ data (Fig. 2a, right axis) for $100 \text{ K} < T < 300 \text{ K}$ yields an effective moment $\mu_{\text{eff}} = 2.18 \mu_B$ and a Weiss temperature $\theta_W = -85 \text{ K}$. The relatively large value of the effective moment is a signature of fluctuating Fe moments in the paramagnetic state. Moreover, the negative θ_W indicates that the dominant interactions between the moments are antiferromagnetic. At low temperatures, $\chi(T)$ presents a weak shoulder at around 50 K, followed by a broad peak centered around 6 K. The specific heat data also show a rounded peak at around 6 K, corresponding to the anomaly in $\chi(T)$ (see Fig. 2b). However, there is no evident feature in $C_p(T)$ at $T \approx 50 \text{ K}$, making the presence of any phase transition in this temperature range unlikely. The rounded nature of the anomalies in susceptibility and specific heat at $T \approx 6 \text{ K}$ point to short-range magnetic order.

In the inset of Fig. 2b the specific-heat data are plotted as $C_p(T)/T$ vs. T^2 . The linear region observed between 20 and 35 K was fitted with $C_p(T) = \gamma T + \beta T^3$ to obtain the Sommerfeld coefficient $\gamma = 150 \text{ mJ/molK}^2$. This is a very large value for a transition metal compound, indicating very strong electronic correlation effects. Using the γ value and the low-temperature susceptibility, we obtain a Sommerfeld-Wilson ratio $R_W = (\pi^2 k_B^2 \chi_{1.8\text{K}}) / (\mu_{\text{eff}} \gamma)$ of 4.9, which is enhanced compared to $R_W = 1$ for the free-electron gas. The enhanced Sommerfeld-Wilson ratio in-

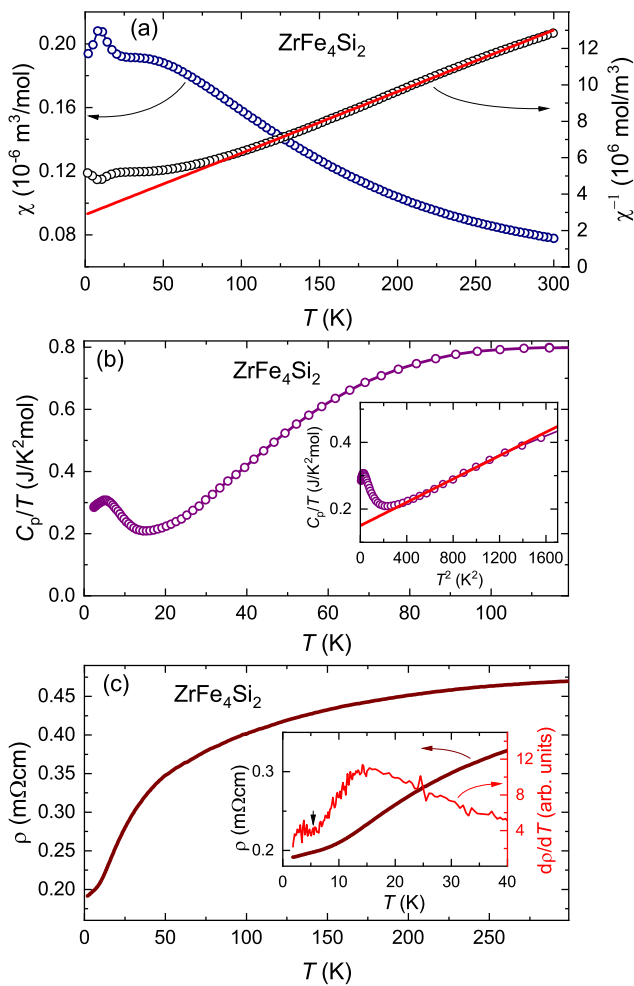


FIG. 2: (a) Temperature dependence of the DC magnetic susceptibility $\chi(T)$ of ZrFe_4Si_2 (left axis). The intrinsic susceptibility is obtained by removing the FM impurity contribution, as explained in the main text. The inverse magnetic susceptibility $\chi^{-1}(T)$ is shown on the right axis. The red curve is the Curie-Weiss fit to the data in the temperature interval between 100 and 300 K. (b) Temperature dependence of the specific heat of ZrFe_4Si_2 plotted as C_p/T vs. T . The inset shows C_p/T vs. T^2 , where the red line is a linear fit to the data between 20 and 35 K. (c) Temperature dependence of the electrical resistivity $\rho(T)$ of ZrFe_4Si_2 . Inset: an enlarged view of the low temperature region of the $\rho(T)$ curve (left axis) along with the temperature derivative $d\rho(T)/dT$ (right axis).

indicates the presence of strong electron-electron magnetic correlations in ZrFe_4Si_2 .

The temperature dependence of the electrical resistivity $\rho(T)$ of ZrFe_4Si_2 is shown in Fig. 2c. $\rho(T)$ decreases monotonically upon cooling with a strong negative curvature below 100 K, probably originating from strong magnetic correlations. Preliminary Mössbauer and muon-spin relaxation (μSR) experiments indicate the onset of dynamic correlations below 100 K and the onset of weak static magnetic order below 8 K²⁵. At low temperatures,

$\rho(T)$ presents only an extremely weak feature around 6 K, as seen in the temperature derivative of the resistivity $d\rho(T)/dT$ plotted in the inset of Fig. 2c. Such a weak anomaly in resistivity is also consistent with short-range magnetic order.

It is also important to note that, unlike other compounds in the $A\text{Fe}_4X_2$ family with trivalent A which show a structural transition associated with the magnetic ordering, temperature-dependent PXRD data do not resolve any structural transition in ZrFe_4Si_2 around 6 K²⁶. Therefore, the low temperature properties of ZrFe_4Si_2 are not related to a structural phase transition.

B. Tuning the ground state of ZrFe_4Si_2 by Ge substitution

The weak, short-range ordered magnetic ground state in ZrFe_4Si_2 raises the question of whether the material is situated close to a QCP connected to the disappearance of long-range magnetic order, especially since such long-range order has been observed in other members of the 142 family^{22,23}. To investigate this possibility, we have carried out a Ge substitution study. As Ge is larger than Si, varying the Ge content in $\text{ZrFe}_4(\text{Si}_{1-x}\text{Ge}_x)_2$ provides a tuning parameter for systematically increasing the unit-cell volume.

To this end, polycrystalline samples of $\text{ZrFe}_4(\text{Si}_{1-x}\text{Ge}_x)_2$ with Ge concentrations $x = 0.12, 0.23, 0.34,$ and 0.46 were synthesized, and their magnetic properties were studied using various physical probes. We note that our attempts to synthesize samples with $x = 0.5$ and 0.6 resulted in phase separation, indicating that compounds with large Ge content are unstable. This is corroborated by the fact that, to our knowledge, pure ZrFe_4Ge_2 has not been reported in the literature.

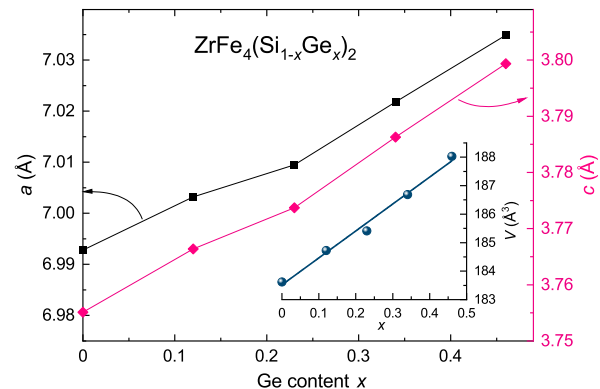


FIG. 3: Lattice parameters a (left axis) and c (right axis) of the investigated $\text{ZrFe}_4(\text{Si}_{1-x}\text{Ge}_x)_2$ samples plotted against their Ge content x . The inset shows the change in the lattice volume V with Ge substitution. The solid line in the inset is a linear fit to the data.

Figure 3 depicts the change in the lattice parameters of $\text{ZrFe}_4(\text{Si}_{1-x}\text{Ge}_x)_2$ with increasing Ge content x , ex-

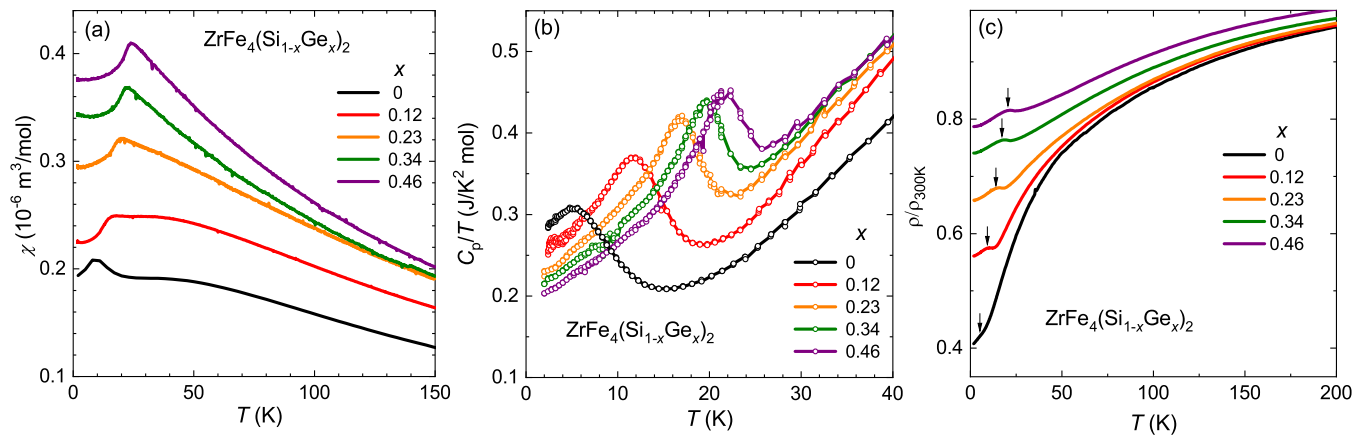


FIG. 4: Temperature dependence of (a) DC magnetic susceptibility $\chi(T)$, (b) specific heat $C_p(T)/T$, and (c) normalized electrical resistivity $\rho(T)/\rho_{300\text{K}}$ of $\text{ZrFe}_4(\text{Si}_{1-x}\text{Ge}_x)_2$ for several Ge concentrations. The intrinsic susceptibility was obtained by removing the FM impurity contribution, as explained in the main text. The position of the peak maxima in the $\chi(T)$ and $C_p(T)/T$ data were taken as the transition temperatures. Corresponding resistive transition temperatures, estimated from the minima in the temperature derivative $d\rho(T)/dT$, are marked by the arrows.

tracted from PXRD measurements. Lattice parameters a (left axis) and c (right axis) monotonically increase with increasing Ge content. Ge substitution with $x = 0.46$ results in an increase of a and c by 0.6% and 1.2%, respectively. The unit-cell volume V increases nearly linearly, reaching a 2.4% increase for the compound with $x = 0.46$ (see the inset of Fig. 3). These results confirm that, as expected, the unit-cell volume of $\text{ZrFe}_4(\text{Si}_{1-x}\text{Ge}_x)_2$ continuously increases with Ge substitution.

The physical properties of $\text{ZrFe}_4(\text{Si}_{1-x}\text{Ge}_x)_2$ with different Ge concentrations were investigated using magnetization, specific heat, and electrical-resistivity measurements. The temperature dependence of magnetic susceptibility is shown in Fig. 4a. The samples in the substitution series contain up to 5% impurity phases of $\text{Fe}_3(\text{Si}_{1-x}\text{Ge}_x)$, which order ferromagnetically between 800 K and 600 K^{24,27}. Their temperature independent, saturated magnetization contribution M_{FM} was subtracted to obtain the intrinsic susceptibility $\chi(T) = [M(T) - M_{\text{FM}}]/H$. As discussed earlier, $\chi(T)$ of the stoichiometric ZrFe_4Si_2 sample has a broad shoulder at about 50 K and a small anomaly around 6 K. The shoulder-like feature at 50 K becomes weaker for the $x = 0.12$ and 0.23 samples and eventually vanishes for $x = 0.34$. The anomaly corresponding to the short-range magnetic order in ZrFe_4Si_2 shifts to higher temperatures upon increasing Ge content. Moreover, the anomaly develops into a cusp-like feature indicating long-range antiferromagnetic ordering in compounds with larger Ge contents. These results are confirmed by the specific-heat data presented in Fig. 4b. The peak in $C_p(T)/T$ shifts to higher temperatures and sharpens with increasing Ge content, with the transition temperature T_N reaching 23 K at $x = 0.46$. In the Ge-substituted samples, the anomaly in $C_p(T)/T$ resembles a mean-field-type transition into a long-range ordered phase. We further note

that the $C_p(T)/T$ values at the lowest temperatures remain large, in the range of 200 – 300 mJ/K²mol. Thus the Sommerfeld coefficient stays large in the whole concentration range, confirming the presence of strong electronic correlations.

The temperature dependent resistivity data $\rho(T)/\rho_{300\text{K}}$ provide further details on the nature of the magnetic ordering (see Fig. 4c). Already at a low Ge substitution level of $x = 0.12$, the $\rho(T)/\rho_{300\text{K}}$ curve shows a noticeable upturn around 11 K, reminiscent of a SDW transition. The increase in resistivity is attributed to the formation of an energy gap at part of the Fermi surface due to the SDW formation. With increasing Ge content, the upturn in resistivity becomes much more pronounced and shifts to higher temperatures. These results reveal that Ge substitution stabilizes the weak short-range magnetic order in ZrFe_4Si_2 into a long-range SDW-type magnetic order.

C. Tuning $\text{ZrFe}_4(\text{Si}_{0.88}\text{Ge}_{0.12})_2$ by hydrostatic pressure

The previous results from the Ge substitution in $\text{ZrFe}_4(\text{Si}_{1-x}\text{Ge}_x)_2$ study show that application of negative chemical pressure stabilizes the magnetic order in $\text{ZrFe}_4(\text{Si}_{1-x}\text{Ge}_x)_2$. This leads to the expectation that external hydrostatic pressure suppresses the magnetic order and eventually drives the system toward an antiferromagnetic QCP. In order to study this, we performed electrical-resistivity measurements under external pressure. We decided to use the slightly Ge substituted compound $\text{ZrFe}_4(\text{Si}_{0.88}\text{Ge}_{0.12})_2$ for the pressure study since the anomaly in the electrical resistivity of ZrFe_4Si_2 is only weak and we do not have a well-developed long-range ordered state. In contrast to that, our data for

$\text{ZrFe}_4(\text{Si}_{0.88}\text{Ge}_{0.12})_2$ indicate long-range SDW order and show a clear anomaly in $\rho(T)$ corresponding to the SDW transition, making it an ideal sample for the pressure experiment. The relatively low $T_N = 11.4$ K for $x = 0.12$ ensures also that moderate pressures will be sufficient to suppress the magnetic order in comparison with compounds with larger Ge concentrations.

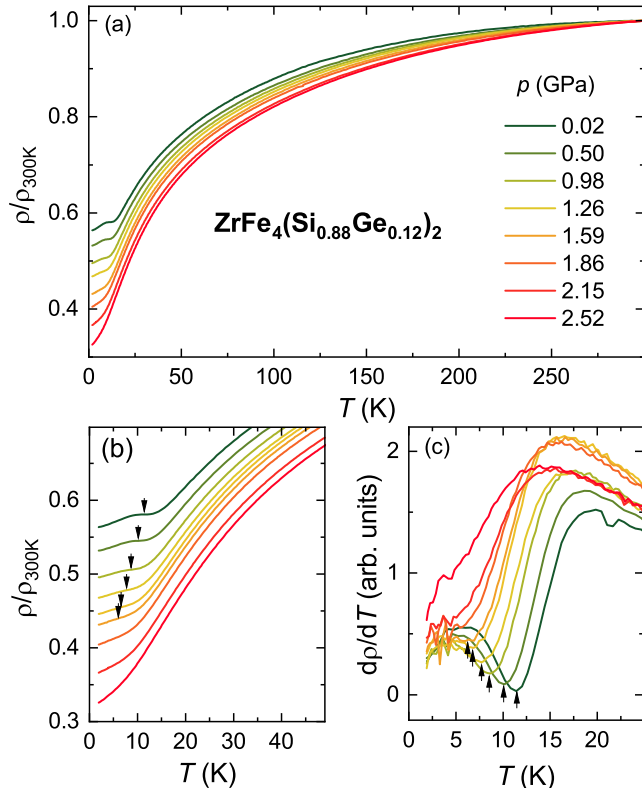


FIG. 5: (a) Normalized electrical resistivity $\rho(T)/\rho_{300\text{K}}$ of $\text{ZrFe}_4(\text{Si}_{0.88}\text{Ge}_{0.12})_2$ as a function of temperature for different applied pressures. (b) Enlarged view of the low temperature region of the $\rho(T)/\rho_{300\text{K}}$ curves. (c) Temperature derivative $d\rho(T)/dT$ vs. T . The arrows indicate the transition temperatures T_N determined by the minima in $d\rho(T)/dT$.

The electrical resistivity of $\text{ZrFe}_4(\text{Si}_{0.88}\text{Ge}_{0.12})_2$ has been investigated under hydrostatic pressures up to $p = 2.5$ GPa and in the temperature range between 2 and 300 K. The curves of the normalized resistivity $\rho(T)/\rho_{300\text{K}}$ for several pressures are plotted in Fig. 5a. One immediately recognizes that pressure has a sizable influence on the temperature dependence of the resistivity. Comparing Fig. 5a with Fig. 4c, it is obvious that applying pressure has the opposite effect of substituting Ge for Si: The curvature in the temperature range between 20 and 300 K increases with pressure, resulting in a larger slope $d\rho(T)/dT$ at 20 K (see also 5c). Since this strong curvature is very likely connected to the onset of dynamical correlations observed in μSR^{25} , applying pressure seemingly strengthens these dynamic correlations. Furthermore, with increasing pressure the anomaly corresponding to the long range order at 11.4 K at ambi-

ent pressure shifts to lower temperatures. This can be better seen in Figs. 5b and 5c, where we plot the low-temperature parts of the resistivity and its temperature derivative $d\rho(T)/dT$. At $p = 0.02$ GPa, a small hump in $\rho(T)$ associated with the SDW transition is observed. The transition temperature T_N is determined from the minimum in the temperature derivative of $\rho(T)$. As pressure is increased, the anomaly in resistivity shifts to lower temperatures, as marked by the arrows. Moreover, the magnitude of the upturn strongly reduces with increase in pressure. The anomaly shifts to 5.2 K at 1.67 GPa. At 1.87 GPa, the anomaly becomes too small and not traceable due to limited resolution of the data in the respective temperature range. At further increased pressures, $\rho(T)$ monotonously decreases upon decreasing temperature without any visible anomaly down to the lowest accessible temperature in our experiments. These results confirm that the SDW transition in $\text{ZrFe}_4(\text{Si}_{0.88}\text{Ge}_{0.12})_2$ is continuously suppressed to zero temperature by external pressure, which suggests the existence of a pressure-tuned QCP.

The magnetoresistance $\text{MR}(H) = [\rho(H) - \rho(0)]/\rho(0)$ of $\text{ZrFe}_4(\text{Si}_{0.88}\text{Ge}_{0.12})_2$ shows marked features connected to the suppression of the magnetic order. Figure 6 depicts $\text{MR}(H)$ measured at $T = 2$ K for several pressures. At low pressures, $\text{MR}(H)$ continuously increases upon increasing field exhibiting a quadratic field dependence, which is typical for a metallic system. For $p \geq 1.59$ GPa, $\text{MR}(H)$ decreases initially upon increasing field, displays a broad minimum and increases again. This contrasting behavior of the MR between the low- and high-pressure regions might be attributed to the enhanced magnetic fluctuations associated with the suppression of the magnetic order. The magnetic field quenches such fluctuations and reduces their scattering contribution, giving rise to the negative MR.

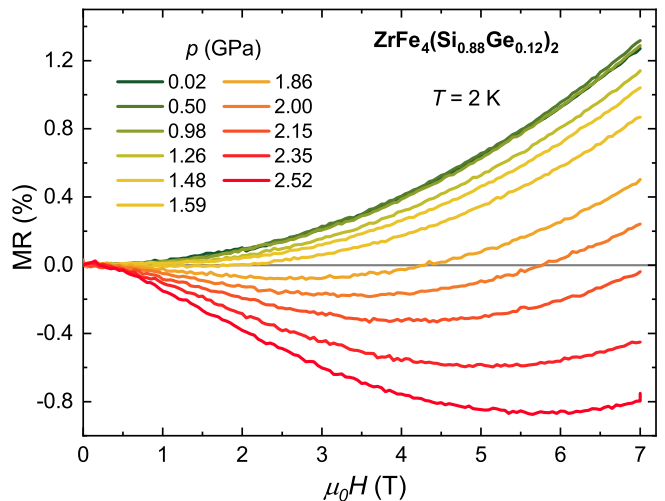


FIG. 6: Magnetic field dependence of the magnetoresistance $\text{MR}(H) = [\rho(H) - \rho(0)]/\rho(0)$ of $\text{ZrFe}_4(\text{Si}_{0.88}\text{Ge}_{0.12})_2$ measured at $T = 2$ K under several applied pressures. The gray line corresponds to $\text{MR} = 0$.

IV. DISCUSSION

The results from the Ge substitution studies in $\text{ZrFe}_4(\text{Si}_{1-x}\text{Ge}_x)_2$ are presented as a temperature–Ge-content phase diagram in Fig. 7a. The transition temperatures T_N obtained from magnetic susceptibility, heat capacity, and electrical resistivity data are plotted. Increasing Ge concentration stabilizes the short-range magnetic order present in ZrFe_4Si_2 into a SDW phase observable in Ge-substituted ZrFe_4Si_2 . $T_N(x)$ is continuously enhanced with increasing Ge content x , reaching 23 K at $x = 0.46$.

As expected, external hydrostatic pressure produces the opposite effect to that of the negative chemical pressure from Ge substitution. The results obtained from the electrical-resistivity measurements on $\text{ZrFe}_4(\text{Si}_{0.88}\text{Ge}_{0.12})_2$ are summarized in the temperature–pressure phase diagram presented in Fig. 7b. At ambient pressure, the compound orders antiferromagnetically at $T_N = 11.4$ K. With increasing pressure, T_N is monotonously suppressed to lower temperatures, reaching 5.2 K at $p = 1.67$ GPa. No traceable anomaly in resistivity can be resolved at higher pressures. However, an extrapolation of the experimental data proposes that the magnetic ordering is suppressed to zero temperature at a critical pressure of $p_c \approx 2.1$ GPa, suggesting the presence of a pressure-tuned antiferromagnetic QCP.

In order to compare the effect of Ge substitution and hydrostatic pressure on the magnetic ordering, it is useful to use the unit-cell volume as a common scale. High-pressure PXRD investigations on isostructural LuFe_4Ge_2 revealed a nearly linear pressure dependence of the lattice volume, yielding a bulk modulus of about 160 GPa²⁸. In ZrFe_4Si_2 a similar pressure dependence of the lattice volume and, therefore, a similar bulk modulus is expected. Thus, we use a bulk modulus of 160 GPa to estimate the lattice volume at different pressures in $\text{ZrFe}_4(\text{Si}_{0.88}\text{Ge}_{0.12})_2$. The transition temperatures determined from electrical-resistivity data of the Ge substitution series and that of $\text{ZrFe}_4(\text{Si}_{0.88}\text{Ge}_{0.12})_2$ under hydrostatic pressure are plotted against the unit-cell volume V in the combined temperature–lattice-volume phase diagram shown in Fig. 7c. The change in T_N with Ge substitution and with hydrostatic pressure is rather consistent and evidences the lattice volume as the governing control parameter. Furthermore, T_N shows a continuous suppression of the magnetic ordering with decreasing lattice volume toward a putative antiferromagnetic QCP at $V \approx 182 \text{ \AA}^3$.

A highly debated question is whether the Fermi liquid behavior expected for a metal at low temperatures breaks down at a QCP, resulting in a non-Fermi liquid (NFL). In the electrical resistivity an NFL is characterized by a deviation from the quadratic dependence of $\rho(T)$ at low temperatures ($\rho = \rho_0 + AT^n$, $n < 2$), which is expected for a Fermi liquid. Our data in the temperature range down to 2 K seem to indicate a temperature exponent smaller than 2 close to p_c and a recovery of Fermi

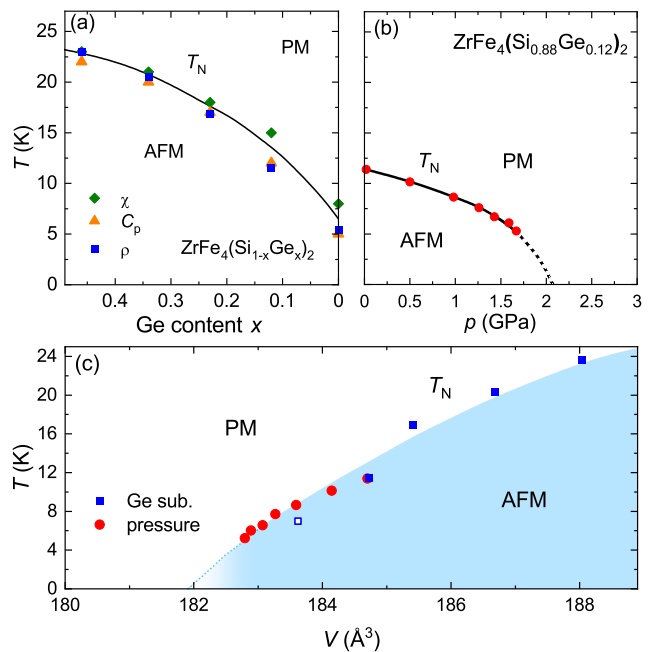


FIG. 7: (a) Temperature vs. Ge-content phase diagram. T_N determined from magnetic-susceptibility, heat-capacity, and electrical-resistivity data are included. (b) Temperature–pressure phase diagram of $\text{ZrFe}_4(\text{Si}_{0.88}\text{Ge}_{0.12})_2$ determined from the electrical-resistivity data. (c) Temperature–lattice volume phase diagram showing T_N determined from electrical resistivity data from both Ge substitution and high-pressure studies. The open symbol corresponds to the weak anomaly observed in ZrFe_4Si_2 . The solid lines are guide to the eyes. The dashed line is an extrapolation to the experimental data.

liquid behavior ($n = 2$) at higher pressures. However, these data give only a first hint. The temperature exponent $n = d \ln(\rho - \rho_0) / d(\ln T)$ shows a significant temperature dependence in the low-temperature region for all pressures. In addition, the increased noise in the low-temperature data makes the accurate determination of the exponent difficult. These first results indicate that experiments at lower temperatures are highly desirable.

Magnetic QCPs in transition metal systems are, meanwhile, a well-established research topic. Early cases were the ferromagnetic systems ZrZn_2 and NbFe_2 ^{29,30}. Presently, the most prominent examples are certainly the Fe pnictides and chalcogenides because there the disappearance of an antiferromagnetic (AFM) state results in the onset of unconventional superconductivity^{31,32}. It is therefore interesting to compare ZrFe_4Si_2 with well-studied transition metal systems close to a magnetic QCP. The T -dependence of the susceptibility, with Curie-Weiss behavior at high temperatures and a leveling out or maximum at lower temperatures is common in transition metal systems close to a QCP. Also the T -dependence of the resistivity, with a pronounced negative curvature in the range 20 – 100 K is common in such systems. However, there is one property where ZrFe_4Si_2 stands out in comparison to most itin-

erant transition metal systems: it presents a huge Sommerfeld coefficient. In transition metal systems, QCPs do not necessarily result in large γ values. In the prototypical system BaFe_2As_2 , e.g., γ reaches only a value of 5 mJ/molK^2 in the stoichiometric system and values of about 25 mJ/molK^2 at the substitution-induced QCP^{33,34}. In ZrFe_4Si_2 , the value $\gamma = 150 \text{ mJ/molK}^2$ deduced from the high-temperature ($> 20 \text{ K}$) extrapolation (see Fig. 2b) is already one order of magnitude larger, and far above the values typically observed in transition metal systems, even close to a QCP. Furthermore this extrapolated γ value obviously misses a large part of the low energy excitations, since the C_p/T value at the lowest investigated temperature of 2 K is significantly larger, about 290 mJ/molK^2 . The evolution of C_p/T at 2 K as a function of Ge content evidences this value to present a maximum at or near the putative QCP. To our knowledge, within transition metal systems, the value of 290 mJ/molK^2 is only surpassed in the compound LiV_2O_4 , which presents a C_p/T value of 420 mJ/molK^2 at low temperature³⁵⁻³⁷. Several mechanisms have been invoked to explain the huge C_p/T value in LiV_2O_4 ³⁸⁻⁴². All invoke strong geometrical frustration due to V atoms forming a pyrochlore sublattice. Notably, in many of the further itinerant systems presenting a very large γ value, there is compelling evidence for strong frustration too, as e.g., in YMn_2 ($\gamma = 180 \text{ mJ/molK}^2$)⁴³, Mn_3P ($\gamma = 100 \text{ mJ/molK}^2$)⁴⁴, and $\beta\text{-Mn}$ ($\gamma = 70 \text{ mJ/molK}^2$)⁴⁵. There is a second family of transition metal systems showing a large Sommerfeld coefficient, which includes e.g. CsFe_2As_2 ($\gamma = 184 \text{ mJ/molK}^2$)⁴⁶, $\text{Ca}_{2-x}\text{Sr}_x\text{RuO}_4$ ($\gamma = 250 \text{ mJ/molK}^2$)⁴⁷, and $\text{CaCu}_3\text{Ir}_4\text{O}_{12}$ ($\gamma = 175 \text{ mJ/molK}^2$)⁴⁸, but there the large γ coefficient is suggested to originate from the closeness to a Mott transition. For ZrFe_4Si_2 , the evolution of the resistivity as a function of Ge substitution or pressure makes this scenario rather unlikely since it indicates the system becomes more metallic when approaching the QCP. Thus the huge electronic specific heat observed at low temperature in ZrFe_4Si_2 compared to values in transition metal systems supports frustration being relevant in ZrFe_4Si_2 . Already in the context of YMn_2 , Pinettes and Lacroix demonstrated that frustration can strongly enhance the γ coefficient close to a QCP in an itinerant system³⁹.

V. SUMMARY

In conclusion, we have investigated ZrFe_4Si_2 using magnetization, thermodynamic, and electrical-transport

measurements and tuned its ground-state properties by Ge substitution and by application of hydrostatic pressure. In the crystal structure of ZrFe_4Si_2 the Fe tetrahedra are prone to magnetic frustration, and their chain-like arrangement represent a quasi-one-dimensional magnetic system, a combination which is expected to enhance quantum fluctuations. Despite having large paramagnetic Fe moments ($\mu_{\text{eff}} = 2.18 \mu_B$) with dominantly antiferromagnetic interactions, ZrFe_4Si_2 shows short-range magnetic order below 6 K . Ge substitution on the Si sites acts as a negative chemical pressure and stabilizes the short-range magnetic order into a long-range spin-density wave order. By applying hydrostatic pressure on $\text{ZrFe}_4(\text{Si}_{0.88}\text{Ge}_{0.12})_2$ we continuously suppressed the magnetic order to zero temperature, as shown by the electrical-resistivity data. Therefore, our combined chemical substitution and hydrostatic pressure study suggests the presence of a lattice-volume controlled antiferromagnetic quantum critical point in ZrFe_4Si_2 . In the hydrostatic pressure experiment on $\text{ZrFe}_4(\text{Si}_{0.88}\text{Ge}_{0.12})_2$ we can infer a critical pressure $p_c \approx 2.1 \text{ GPa}$ and, indeed, magnetoresistance data indicate enhanced magnetic fluctuations associated with the suppression of the magnetic order. Moreover, zero-field resistivity data point to a breakdown of the Fermi liquid description in the vicinity of p_c . In comparison to other transition metal systems, ZrFe_4Si_2 presents a large specific heat at low temperatures, reaching a C_p/T value of 290 mJ/molK^2 at 2 K . This large electronic specific heat at low temperatures supports the relevance of magnetic frustration in ZrFe_4Si_2 . Therefore our results evidence ZrFe_4Si_2 as a strongly correlated electron system with a constellation of interesting properties and thus worth being investigated in depth.

Acknowledgment

This work was partly supported by Deutsche Forschungsgemeinschaft (DFG) through the Research Training Group GRK 1621.

* Electronic address: ajeesh@cpfs.mpg.de

¹ H. Kotegawa and M. Fujita, Magnetic excitations in iron chalcogenide superconductors, *Sci. Technol. Adv. Mater.* **13**, 054302 (2012).

² P. Dai, Antiferromagnetic order and spin dynamics in iron-

based superconductors, *Rev. Mod. Phys.* **87**, 855 (2015).

³ D. S. Inosov, Spin fluctuations in iron pnictides and chalcogenides: From antiferromagnetism to superconductivity, *C. R. Physique* **17**, 60 (2016).

⁴ S. Chi, R. Aluru, S. Grothe, A. Kreisel, U. R. Singh, B.

- M. Andersen, W. N. Hardy, R. Liang, D. A. Bonn, S. A. Burke, and P. Wahl, Imaging the real space structure of the spin fluctuations in an iron-based superconductor, *Nat. Commun.* **8**, 15996 (2017).
- 5 P. J. Hirschfeld, Using gap symmetry and structure to reveal the pairing mechanism in Fe-based superconductors, *C. R. Physique* **17**, 197 (2016).
 - 6 S. R. Julian, F. V. Carter, F. M. Grosche, R. K. W. Haselwimmer, S. J. Lister, N. D. Mathur, G. J. McMullan, C. Pfleiderer, S. S. Saxena, I. R. Walker, N. J. W. Wilson, and G. G. Lonzarich, Non-Fermi-liquid behaviour in magnetic d - and f -electron systems, *J. Magn. Magn. Mater.* **177–181**, 265 (1998).
 - 7 G. R. Stewart, Non-Fermi-liquid behavior in d - and f -electron metals, *Rev. Mod. Phys.* **73**, 797 (2001).
 - 8 H. v. Löhneysen, A. Rosch, M. Vojta, and P. Wölfle, Fermi-liquid instabilities at magnetic quantum phase transitions, *Rev. Mod. Phys.* **79**, 1015 (2007).
 - 9 B. Shen, Y. Zhang, Y. Komijani, M. Nicklas, R. Borth, A. Wang, Y. Chen, Z. Nie, R. Li, X. Lu, H. Lee, M. Smidman, F. Steglich, P. Coleman, and H. Yuan, Strange-metal Behaviour in a Pure Ferromagnetic Kondo Lattice, *Nature* **579**, 51 (2020).
 - 10 Ya. P. Yarmoluk, L. A. Lysenko, and E. I. Gladyshevski, *Dopov. Akad. Nauk Ukr. RSR, Ser. A* **37**, 279 (1975).
 - 11 P. Schobinger-Papamantellos, J. Rodriguez-Carvajal, G. Andre, C. H. de Groot, F. R. de Boer, and K. H. J. Buschow, Magnetic ordering of ErFe_4Ge_2 studied by neutron diffraction and magnetic measurements, *J. Magn. Magn. Mater.* **191**, 261 (1999).
 - 12 P. Schobinger-Papamantellos, J. Rodriguez-Carvajal, K. H. J. Buschow, E. Dooryhee, and A. N. Fitch, The double-phase transition of ErFe_4Ge_2 : An XRPD study, *J. Magn. Magn. Mater.* **210**, 121 (2000).
 - 13 P. Schobinger-Papamantellos and T. Janssen, The symmetry of the incommensurate magnetic phase of ErFe_4Ge_2 , *Z. Kristallogr.* **221**, 732 (2006).
 - 14 P. Schobinger-Papamantellos, J. Rodriguez-Carvajal, and K. H. J. Buschow, Double symmetry breaking and magnetic transitions in ErFe_4Ge_2 , *J. Magn. Magn. Mater.* **310**, 63 (2007).
 - 15 P. Schobinger-Papamantellos, J. Rodriguez-Carvajal, K. H. J. Buschow, E. Dooryhee, and A. N. Fitch, Magnetostructural phase transitions of DyFe_4Ge_2 : Part I-By XRPD, *J. Magn. Magn. Mater.* **300**, 315 (2006).
 - 16 P. Schobinger-Papamantellos, J. Rodriguez-Carvajal, G. Andre, and K. H. J. Buschow, Magnetostructural phase transitions of DyFe_4Ge_2 : Part II-Neutron diffraction, *J. Magn. Magn. Mater.* **300**, 333 (2006).
 - 17 P. Schobinger-Papamantellos, J. Rodriguez-Carvajal, K. H. J. Buschow, E. Dooryhee, and A. N. Fitch, Re-entrant magneto-elastic transition in HoFe_4Ge_2 : an XRPD study, *J. Magn. Magn. Mater.* **250**, 225 (2002).
 - 18 P. Schobinger-Papamantellos, J. Rodriguez-Carvajal, G. Andre, C. Ritter, and K. H. J. Buschow, Re-entrant magneto-elastic transition in HoFe_4Ge_2 : a neutron diffraction study, *J. Magn. Magn. Mater.* **280**, 119 (2004).
 - 19 P. Schobinger-Papamantellos, K. H. J. Buschow, and J. Rodriguez-Carvajal, Double symmetry breaking in TmFe_4Ge_2 compared to RFe_4Ge_2 ($R = \text{Y, Lu, Er, Ho, Dy}$) magnetic behaviour, *J. Magn. Magn. Mater.* **355**, 104 (2014).
 - 20 J. Liu, D. Paudyal, Y. Mudryk, J. D. Zou, K. A. Gschneidner Jr., and V. K. Pecharsky, Unusual magnetic and structural transformations of DyFe_4Ge_2 , *Phys. Rev. B* **88**, 014423 (2013).
 - 21 J. Liu, V. K. Pecharsky, and K. A. Gschneidner Jr., Multiple phase transitions and magnetoresistance of HoFe_4Ge_2 , *J. Alloys Comp.* **631**, 26 (2015).
 - 22 P. Schobinger-Papamantellos, J. Rodriguez-Carvajal, G. Andre, N. P. Duong, K. H. J. Buschow, and P. Toledano, Simultaneous structural and magnetic transitions in YFe_4Ge_2 studied by neutron diffraction and magnetic measurements, *J. Magn. Magn. Mater.* **236**, 14 (2001).
 - 23 P. Schobinger-Papamantellos, K. H. J. Buschow, and J. Rodriguez-Carvajal, Magnetoelastic phase transitions in the LuFe_4Ge_2 and YFe_4Si_2 compounds: A neutron diffraction study, *J. Magn. Magn. Mater.* **324**, 3709 (2012).
 - 24 T. Shinjo, Y. Nakamura, and N. Shikazono, Magnetic Study of Fe_3Si and Fe_5Si_3 by Mössbauer Effect, *J. Phys. Soc. Japan* **18**, 797 (1963).
 - 25 T. Goltz, N. Mufti, C. Geibel, J. Spehling, H. Luetkens, and H.-H. Klauss, Disentanglement of static and dynamic magnetism in itinerant AFe_4X_2 systems studied by Muon Spin Relaxation and Mössbauer Spectroscopy (DPG Spring Meeting, Berlin, 2012).
 - 26 T. Woike (private communication).
 - 27 K. Kanematsu, K. Yasukochi, and T. Ohoyama, Magnetic Properties and Phase Transition of Fe_3Ge , *J. Phys. Soc. Japan* **18**, 920 (1963).
 - 28 M. O. Ajeesh, S. Dengre, R. Sarkar, P. Materne, K. Weber, R. D. dos Reis, I. Kraft, R. Khasanov, S. Medvedev, V. Ksenofontov, W. Bi, J. Zhao, E. E. Alp, H. Rosner, H.-H. Klauss, C. Geibel, and M. Nicklas (unpublished).
 - 29 B. T. Matthias and R. M. Bozorth, Ferromagnetism of a Zirconium-Zinc Compound, *Phys. Rev.* **109**, 604 (1958).
 - 30 M. Shiga and Y. Nakamura, Magnetic Properties of Stoichiometric and Off-Stoichiometric NbFe_2 , *J. Phys. Soc. Jpn.* **56**, 4040 (1987).
 - 31 Y. Kamihara, T. Watanabe, M. Hirano, and H. Hosono, Iron-Based Layered Superconductor $\text{La}[\text{O}_{1-x}\text{F}_x]\text{FeAs}$ ($x = 0.05 - 0.12$) with $T_c = 26$ K, *J. Am. Chem. Soc.* **130**, 3296 (2008).
 - 32 D. C. Johnston, The puzzle of high temperature superconductivity in layered iron pnictides and chalcogenides, *Advances in Physics* **59**, 803 (2010).
 - 33 F. Hardy, P. Burger, T. Wolf, R. A. Fisher, P. Schweiss, P. Adelman, R. Heid, R. Fromknecht, R. Eder, D. Ernst, H. v. Löhneysen, and C. Meingast, Doping evolution of superconducting gaps and electronic densities of states in $\text{Ba}(\text{Fe}_{1-x}\text{Co}_x)_2\text{As}_2$ iron pnictides, *EPL* **91**, 47008 (2010).
 - 34 A. E. Böhrer, P. Burger, F. Hardy, T. Wolf, P. Schweiss, R. Fromknecht, H. v. Löhneysen, C. Meingast, H. K. Mak, R. Lortz, S. Kasahara, T. Terashima, T. Shibauchi, and Y. Matsuda, Thermodynamic phase diagram, phase competition, and uniaxial pressure effects in $\text{BaFe}_2(\text{As}_{1-x}\text{P}_x)_2$ studied by thermal expansion, *Phys. Rev. B* **86**, 094521 (2012).
 - 35 S. Kondo, D. C. Johnston, C. A. Swenson, F. Borsa, A. V. Mahajan, L. L. Miller, T. Gu, A. I. Goldman, M. B. Maple, D. A. Gajewski, E. J. Freeman, N. R. Dilley, R. P. Dickey, J. Merrin, K. Kojima, G. M. Luke, Y. J. Uemura, O. Chmaissem, and J. D. Jorgensen, LiV_2O_4 : a heavy fermion transition metal oxide, *Phys. Rev. Lett.* **78**, 3729 (1997).
 - 36 C. Urano, M. Nohara, S. Kondo, F. Sakai, H. Takagi, T. Shiraki, and T. Okubo, LiV_2O_4 spinel as a heavy-mass

- Fermi liquid: anomalous transport and role of geometrical frustration, *Phys. Rev. Lett.* **85**, 1052 (2000).
- ³⁷ M. Brando, N. Büttgen, V. Fritsch, J. Hemberger, H. Kaps, H.-A. Krug von Nidda, M. Nicklas, K. Pucher, W. Trinkl, A. Loidl, E.W. Scheidt, M. Klemm, and S. Horn, Ground-state properties of LiV_2O_4 and $\text{Li}_{1-x}\text{Zn}_x(\text{V}_{1-y}\text{Ti}_y)_2\text{O}_4$, *Eur. Phys. J. B* **25**, 289 (2002).
- ³⁸ V. I. Anisimov, M. A. Korotin, M. Zöfl, T. Pruschke, K. Le Hur, and T. M. Rice, Electronic Structure of the Heavy Fermion Metal LiV_2O_4 , *Phys. Rev. Lett.* **83**, 364 (1999).
- ³⁹ C. Pinettes and C. Lacroix, A model for the heavy-fermion behaviour of YMn_2 : influence of frustration on the spin fluctuation spectrum, *J. Phys.: Condens. Matter* **6**, 10093 (1994).
- ⁴⁰ S. Burdin, D. R. Grempel, and A. Georges, Heavy-fermion and spin-liquid behaviour in a Kondo lattice with magnetic frustration, *Phys. Rev. B* **66**, 045111 (2002).
- ⁴¹ H. Kusunose, S. Yotsuhashi, and K. Miyake, Formation of a heavy quasiparticle state in the two-band Hubbard model, *Phys. Rev. B* **62**, 4403 (2000).
- ⁴² Y. Yamashita and K. Ueda, Spin-orbital fluctuations and a large mass enhancement in LiV_2O_4 , *Phys. Rev. B* **67**, 195107 (2003).
- ⁴³ M. Shiga, K. Fujisawa, and H. Wada, Spin Liquid Behavior of Highly Frustrated $\text{Y}(\text{Sc})\text{Mn}_2$ and Effects of Nonmagnetic Impurity, *J. Phys. Soc. Japan.* **62**, 1329 (1993).
- ⁴⁴ H. Kotegawa, M. Matsuda, F. Ye, Y. Tani, K. Uda, Y. Kuwata, H. Tou, E. Matsuoka, H. Sugawara, T. Sakurai, H. Ohta, H. Harima, K. Takeda, J. Hayashi, S. Araki, and T. C. Kobayashi, Helimagnetic Structure and Heavy-Fermion-Like Behavior in the Vicinity of the Quantum Critical Point in Mn_3P , *Phys. Rev. Lett.* **124**, 087202 (2020).
- ⁴⁵ H. Nakamura, K. Yoshimoto, M. Shiga, M. Nishi, and K. Kakurai, Strong antiferromagnetic spin fluctuations and the quantum spin-liquid state in geometrically frustrated $\beta\text{-Mn}$, and the transition to a spin-glass state caused by non-magnetic impurity, *J. Phys.: Condens. Matter* **9**, 4701 (1997).
- ⁴⁶ Y. P. Wu, D. Zhao, A. F. Wang, N. Z. Wang, Z. J. Xiang, X. G. Luo, T. Wu, and X. H. Chen, Emergent Kondo Lattice Behavior in Iron-Based Superconductors AFe_2As_2 ($A = \text{K}, \text{Rb}, \text{Cs}$), *Phys. Rev. Lett.* **116**, 147001 (2016).
- ⁴⁷ S. Nakatsuji, D. Hall, L. Balicas, Z. Fisk, K. Sugahara, M. Yoshioka, and Y. Maeno, Heavy-Mass Fermi Liquid near a Ferromagnetic Instability in Layered Ruthenates, *Phys. Rev. Lett.* **90**, 137202 (2003).
- ⁴⁸ J.-G. Cheng, J.-S. Zhou, Y.-F. Yang, H. D. Zhou, K. Matsumabayashi, Y. Uwatoko, A. MacDonald, and J. B. Goodenough, Possible Kondo Physics near a Metal-Insulator Crossover in the A-Site Ordered Perovskite $\text{CaCu}_3\text{Ir}_4\text{O}_{12}$, *Phys. Rev. Lett.* **111**, 176403 (2013).